

# CNS Distribution of Members of the Two-Pore-Domain (KCNK) Potassium Channel Family

Edmund M. Talley,<sup>1</sup> Guillermo Solórzano,<sup>1</sup> Qiubo Lei,<sup>1</sup> Donghee Kim,<sup>2</sup> and Douglas A. Bayliss<sup>1</sup>

<sup>1</sup>Department of Pharmacology, University of Virginia, Charlottesville, Virginia 22908, and <sup>2</sup>Department of Physiology and Biophysics, Finch University of Health Sciences, The Chicago Medical School, North Chicago, Illinois 60064

Two-pore-domain potassium ( $K^+$ ) channels are substrates for resting  $K^+$  currents in neurons. They are major targets for endogenous modulators, as well as for clinically important compounds such as volatile anesthetics. In the current study, we report on the CNS distribution in the rat and mouse of mRNA encoding seven two-pore-domain  $K^+$  channel family members: TASK-1 (KCNK3), TASK-2 (KCNK5), TASK-3 (KCNK9), TREK-1 (KCNK2), TREK-2 (KCNK10), TRAAK (KCNK4), and TWIK-1 (KCNK1). All of these genes were expressed in dorsal root ganglia, and for all of the genes except TASK-2, there was a differential distribution in the CNS. For TASK-1, highest mRNA accumulation was seen in the cerebellum and somatic motoneurons. TASK-3 was much more widely distributed, with robust expression in all brain regions, with particularly high expression in somatic motoneurons, cerebellar granule neu-

rons, the locus ceruleus, and raphe nuclei and in various nuclei of the hypothalamus. TREK-1 was highest in the striatum and in parts of the cortex (layer IV) and hippocampus (CA2 pyramidal neurons). mRNA for TRAAK also was highest in the cortex, whereas expression of TREK-2 was primarily restricted to the cerebellar granule cell layer. There was widespread distribution of TWIK-1, with highest levels in the cerebellar granule cell layer, thalamic reticular nucleus, and piriform cortex. The differential expression of each of these genes likely contributes to characteristic excitability properties in distinct populations of neurons, as well as to diversity in their susceptibility to modulation.

**Key words:** potassium channel; *in situ* hybridization; KCNK; TASK; TREK; TRAAK; TWIK

As their name suggests, “leak” potassium ( $K^+$ ) channels are  $K^+$ -selective and show relatively little time and voltage dependence. In neurons, they are a major determinant not only of membrane potential but also membrane input resistance, which is a primary factor in the magnitude and kinetics of responses to synaptic inputs. Thus, they are a key component in shaping the characteristics of neuronal excitability.

A family of genes (designated KCNK by the Human Genome Organization) that gives rise to leak  $K^+$  channels has been identified, and over the last few years, a number of the family members have been cloned and characterized (for review, see Lesage and Lazdunski, 2000; Goldstein et al., 2001; Patel and Honore, 2001). These “two-pore-domain”  $K^+$  channels are named for their predicted membrane topology, which entails four transmembrane-spanning regions surrounding two pore-forming loops. They differ structurally from members of the other major potassium channel families [the voltage-gated ( $K_V$ ) and inwardly rectifying ( $K_{IR}$ )  $K^+$  channels], which consist of subunits that contain only one pore domain each.

Currently, 11 mammalian two-pore-domain  $K^+$  channel family members have been demonstrated to form functional channels at the plasma membrane; of these, eight are expressed at appreciable

levels in the CNS (see Discussion). The physiological similarity of these channels and their rather nondescript properties are suggestive of an invariant background role in cellular function. However, these channels appear to represent important loci for modulation of neuronal output as a result of the actions of a host of endogenous and exogenous agents (for review, see Lesage and Lazdunski, 2000; Goldstein et al., 2001; Patel and Honore, 2001). Such agents include neurotransmitters, common intracellular second messengers, a variety of bioactive lipids, and a number of clinically valuable anesthetic and neuroprotective compounds. Moreover, these channels are subject to regulation by changes in biologically important physicochemical parameters, including variations in temperature, intracellular/extracellular pH, oxygen tension, and changes in osmolarity and/or membrane stretch (for review, see Lesage and Lazdunski, 2000; Goldstein et al., 2001; Patel and Honore, 2001). In addition, there is evidence that one of these channels (TASK-1) is a locus of modulation, in the form of compensatory expression, in neurons of mice with genetic deletions of specific GABA receptor subunits (Brickley et al., 2001).

The fact that these channels are subject to alteration from so many different sources makes them interesting from the standpoint of CNS function. Furthermore, differential modulation is a source of heterogeneity among two-pore-domain  $K^+$  channel family members and is likely to contribute to diversity in pharmacological and physiological properties of CNS neurons. For each of these channels, there are data regarding CNS expression; however, in most cases, there is little detail regarding precise cellular and regional distribution. To further understand the nature of their actions in the CNS, we have localized the expression of seven of the two-pore-domain  $K^+$  channel family members by *in situ* hybridization.

Received May 3, 2001; revised July 3, 2001; accepted July 26, 2001.

This work was supported by National Institutes of Health Grants NS33583 (D.A.B.) and MH12091 (predoctoral fellowship to E.M.T.). We thank Drs. M. B. Harrison, R. L. Stornetta, P. G. Guyenet, and the Information Technology Services at the University of Virginia for providing imaging equipment and support. We also thank Drs. A. T. Gray and M. Lazdunski for gifts of cDNAs.

Correspondence should be addressed to Edmund M. Talley, Department of Pharmacology, University of Virginia Health System, P.O. Box 800735, Charlottesville, VA 22908-0735. E-mail: emt3m@virginia.edu.

Copyright © 2001 Society for Neuroscience 0270-6474/01/217491-15\$15.00/0

## MATERIALS AND METHODS

### Tissue preparation

Adult male rats (200–350 gm) from two strains, Wistar (Harlan, Indianapolis, IN) and Sprague Dawley (Hilltop Lab Animals, Scottsdale, PA), and C57BL/6J mice (The Jackson Laboratory, Bar Harbor, ME) were anesthetized with ketamine–xylazine and decapitated. Brains, spinal cords, and ganglia were removed and frozen on dry ice. Sections (10  $\mu$ m) were thaw mounted onto charged slides (Superfrost Plus; Fisher Scientific, Houston, TX) and stored at  $-80^{\circ}\text{C}$  for *in situ* hybridization. Hybridization was performed as described previously (Talley et al., 2000). Sections were fixed very briefly (5 min) in 4% paraformaldehyde, rinsed repeatedly in PBS, treated successively with glycine (0.2% in PBS) and acetic anhydride (0.25% in 0.1 M triethanolamine, 0.9% saline, pH 8), and dehydrated in a graded series of ethanol and chloroform. Hybridization was performed overnight at  $60^{\circ}\text{C}$  in a buffer of 50% formamide, 4 $\times$  SSC (1 $\times$  SSC: 150 mM NaCl and 15 mM sodium citrate, pH 7), 1 $\times$  Denhardt's solution (0.02% each of Ficoll, polyvinylpyrrolidone, and bovine serum albumin), 10% dextran sulfate, 100 mM DTT, 250  $\mu$ g/ml yeast tRNA, and 0.5 mg/ml salmon testes DNA. After hybridization, slides were washed through two changes of 4 $\times$  SSC, treated with RNase A (50  $\mu$ g/ml), washed again through two changes each of 2 $\times$  SSC and 0.5 $\times$  SSC, and finally subjected to a high-stringency wash of 0.1 $\times$  SSC. Each of these washes lasted 20–30 min. They were performed at  $37^{\circ}\text{C}$  and included 10 mM sodium thiosulfate, with the exception of the high-stringency wash, which was performed at  $55^{\circ}\text{C}$  (no sodium thiosulfate). In control experiments, the high-stringency wash was performed at different temperatures and included 25% formamide (see below).

### Radioactive probes

cRNA probes were transcribed using SP6 or T7 RNA polymerase, as indicated, in the presence of [ $\alpha$ - $^{32}\text{P}$ ]UTP. The templates for transcription were as follows.

**TASK-1.** The coding region of rat TASK-1 [obtained from A. T. Gray (University of California, San Francisco, CA); GenBank accession number AF031384; Leonoudakis et al., 1998] was ligated into pcDNA3 (Invitrogen, San Diego, CA) using *EcoRI* and *ApaI*, and linearized with *HindIII* for transcription using SP6 RNA polymerase. A corresponding sense probe was produced by linearizing with *EcoRI* and transcribing with T7.

**TASK-2.** A mouse clone corresponding to the coding region of TASK-2 was obtained by PCR using an expressed sequence tag clone as a template (GenBank accession number AW321680; obtained from Incyte Genomics, St. Louis, MO) and ligated into pcDNA3 using *BamHI* and *XhoI*. The resulting construct was cut with *HindIII* and transcribed with SP6. A corresponding sense probe was generated by linearizing with *XhoI* and transcribing with T7.

**TASK-3.** The coding region of rat TASK-3 was produced by PCR using cloned TASK-3 cDNA as a template (GenBank accession number AF192366; Kim et al., 2000) and ligated into pcDNA3 using *BamHI* and *EcoRI*. The resulting construct was cut with *HindIII* and transcribed with SP6. A corresponding sense probe was generated by linearizing with *EcoRV* and transcribing with T7.

**TREK-1.** cDNA for TREK-1 was generated by PCR from reverse-transcribed mouse cerebellar RNA using primers from the sequence originally identified as the mouse TREK-1 coding region (GenBank accession number U73488.1; nucleotides 484–1596; Fink et al., 1996). This PCR product was ligated into pCRII (Invitrogen); the resulting construct lacks the final 90 nucleotides from the C-terminal end of the revised TREK-1 coding region (GenBank accession number U73488.2). The construct was linearized using *XhoI* and transcribed using SP6.

**TREK-2.** A *HindIII*–*EcoRI* fragment of rat TREK-2 (GenBank accession number AF196965; Bang et al., 2000) was ligated into pcDNA3 (in reverse orientation); the resulting construct was linearized with *EcoRI* and transcribed with T7. A corresponding sense probe was generated by linearizing with *HindIII* and transcribing with SP6.

**TRAAK.** A mouse clone of TRAAK (obtained from A. T. Gray) corresponding to nucleotides 266–1480 of the published sequence (GenBank accession number AF056492; Fink et al., 1998) was ligated into pcDNA3 using *EcoRI* and *XhoI*, linearized using *HindIII*, and transcribed using SP6.

**TWIK-1.** The coding region for human TWIK-1 [obtained from M. Lazdunski (Institut de Pharmacologie Moléculaire et Cellulaire, Valbonne, France); GenBank accession number NM002245; Lesage et al.,

1996] was subcloned into pcDNA3 using *EcoRI* and *XhoI* and linearized with *EcoRI* for transcription with SP6.

### Control experiments

A number of control experiments were performed to establish the specificity of labeling. These included the use of corresponding sense probes (for TASK-1, TASK-2, TASK-3, and TREK-2) and separate experiments using specific oligonucleotide probes (for TASK-1, TREK-1, TRAAK, and TWIK-1). Hybridization with sense probes gave low levels of nonspecific (background) labeling, as expected. Hybridization with oligonucleotide probes resulted in the same set of distribution patterns as the corresponding cRNA probes. The oligonucleotides were as follows: TASK-1, cccccaccagcaggtaggtagagtgacacga, cagaggtgaggaaggcgcgatgaccgtgag, and gactactgcagctctcgcgctctgtaccag (nucleotides 170–138, 829–797, and 1123–1095 of the cloned rat TASK-1; GenBank accession number AF031384; Leonoudakis et al., 1998); TREK-1, cacaatggtgctctctgggaatctctgagg and ggagagcttcgcgttcacggatgtggcacgtg (nucleotides 726–694 and 1536–1504 of the cloned mouse TREK-1; GenBank accession number U73488.2; Fink et al., 1996); TRAAK, gaaatctctccagctctctggtcaccacaggg and ctacaccggcagcgcctt-gtctcgagtgctccc (nucleotides 466–434 and 1480–1448 of the cloned mouse TRAAK; GenBank accession number AF056492; Fink et al., 1998); and TWIK-1, ccaggccgagtgctcaggagatgaaacag and ggccacaaaggctctgttctctctctc (nucleotides 731–699 and 1014–982 of the cloned rat TWIK-1; GenBank accession number AF022819).

To further rule out the possibility of spurious cross-reactivity of the cRNA probes, higher wash stringencies (i.e., final 30 min washes in 0.1 $\times$  SSC and 25% formamide, at  $55^{\circ}\text{C}$ ,  $65^{\circ}\text{C}$ , and  $75^{\circ}\text{C}$ ) were used for control sagittal and horizontal sections. For all probes, these higher-stringency washes resulted in diminished hybridization, but the distribution of labeling was unchanged, indicating that for each probe the same mRNA species was labeled in the various brain regions.

### Data analysis and presentation

All slides were exposed to film (Hyperfilm  $\beta$ -MAX; Amersham Pharmacia Biotech, Arlington Heights, IL) for the same length of time (5 d). The resulting autoradiograms were mounted on a light box and imaged using a video camera (CCD-72; Dage-MTI, Michigan City, IN). The same camera settings were used to generate images from each of the different genes. For resolution of cellular labeling, slides also were dipped in liquid autoradiographic emulsion (NTB2; Eastman Kodak, Rochester, NY), exposed for 5 weeks, and examined by low-power dark-field and high-power bright-field microscopy. Images of silver grains from these slides were captured using the same video camera mounted on a Leitz (Wetzlar, Germany) Diaplan microscope.

Pseudocolor images were rendered using image analysis software (MCID; Imaging Research Inc., St. Catharines, Ontario, Canada) to judge differential intensity of labeling of autoradiograms. Visual inspection of emulsion-dipped slides also was used to identify particular cell types and brain nuclei. Definitions for brain regions and nuclei were established following brain maps and identifying criteria from Paxinos and Watson (Paxinos, 1995; Paxinos and Watson, 1997). A combination of analysis of autoradiograms and emulsion-dipped slides was used to establish a comparative distribution of the transcripts, which is presented as a system of pluses (Table 1), with five pluses (+++++) indicating maximal signal intensity.

## RESULTS

### Overview

*In situ* hybridization was performed on brains and spinal cords using [ $^{32}\text{P}$ ]–labeled cRNA probes specific for seven of the mammalian two-pore-domain K<sup>+</sup> channels. In initial experiments characterizing the probes, horizontal and sagittal brain sections (as well as transverse sections through the spinal cord) were used from two different rat strains, as well as from mice (see Materials and Methods). Transverse sections were taken through the neuraxis from adult Wistar rats; these were used for the figures presented in this report. Information regarding distribution also was verified using horizontal and sagittal sections.

In addition to the brain and spinal cord, sections were taken from dorsal root ganglia, in which all seven of the genes were

**Table 1. Distribution of two-pore-domain K<sup>+</sup> channel mRNA expression in the CNS**

	TASK-1	TASK-3	TREK-1	TREK-2	TRAAK	TWIK-1
<b>Medulla and spinal cord</b>						
Dorsal horn/spinal trigeminal nucleus	++	++	–	+/-	+/-	+/-
Nucleus of the solitary tract	++	++++	++/+++	–	–	–
Cochlear nuclei	++	+/-	–	–	–	++
Somatic motor neurons	++++	+++++	+/-	–	–	–
Reticular fields	++	+/-	–	++/-	–	++
<b>Brainstem aminergic nuclei</b>						
Raphe nuclei	+/+	++++	+/+	+/-	–	–
Substantia nigra	–	–	–	–	–	+/-
Locus ceruleus	+++	+++++	–	–	–	–
<b>Midbrain and cerebellum</b>						
Superior/inferior colliculus	+/-	+/-	+	–	–	+/-
Periaqueductal gray	+/-	++/++++	+	–	–	+/-
Red nucleus	+/-	+++	–	+	–	++
Pontine nuclei	+++	+++	–	+	+/-	++
Interpeduncular nucleus	+++	+++	++	–	–	–
Vestibular nuclei	+/-	+	–	–	–	+/+
Cerebellar granule cell layer	++++	+++++	+	++++	+	++++
<b>Hypothalamus</b>						
Preoptic nuclei	+/+	+++	++/+++	–	+	–
Suprachiasmatic nucleus	+/+	+++++	–	–	+/+	–
Supraoptic nucleus	+/+	+	+	+	+	–
Lateral hypothalamic area	+/+	+/+	+/+	–	–	–
Paraventricular nucleus	+	++	+	–	+/-	–
Arcuate nucleus	++/+++	++++	+++	–	+/-	–
Dorsomedial/ventromedial nuclei	+/+	++/+++++	+/+	–	+/+	–
Mammillary nuclei	+/+	+++/++++	+/-	+/-	+	–
<b>Thalamus</b>						
Principal relay nuclei	+/+	++/+++	–	–	+/+	+/+
Intralaminar nuclei	+/+	+/+	+/-	+/-	+/+	+/+
Reticular nucleus	+/+	+/-	+/+	+	–	+++/++++
Habenula	+	+/+	–	+/-	–	+/++++
<b>Basal forebrain</b>						
Striatum/accumbens	–	-/++++	+++/++++	–	+	+
Olfactory tubercle	+/+	-/++++	+++/++++	+	+	+
Globus pallidus	+/+	+/+	–	–	–	+/+
Subthalamic nucleus	++	+++	–	–	+/-	++
Bed nucleus of the stria terminalis	+/+	++++	+/+	–	+	–
Septum/diagonal band	+/+	+/+	–	–	–	–
<b>Amygdala</b>						
Cortical nuclei	+/+	+/+	+/+	+/+	+/+	+/+
Nucleus of the lateral olfactory tract	+/+	++++	+++	–	++	+
Central nucleus	–	+	+	–	–	–
Medial nucleus	+/+	++/++++	+/+	+/+	+	+
Lateral nucleus	–	+	+/-	+/+	+/+	+/+
Basolateral/basomedial nuclei	–	+	–	–	+/-	+
<b>Hippocampus</b>						
Pyramidal cell layer, CA1	+/+	++	+/+	-/+	++	-/+
Pyramidal cell layer, CA2	+/+	+	++/+++	-/+	++	+/+
Pyramidal cell layer, CA3	+/+	-/+	–	+/+	++	+/+
Granule cell layer, dentate gyrus	+/+	+/++++	+/+	+	++	++
Indusium griseum	+/-	+	+++	–	++	+
<b>Cortex</b>						
Neocortex, layers II/III	+	++/+++	–	-/+	++	++/+++
Neocortex, layer IV	+/+	++	++/+++	-/+	++/+++	++
Neocortex, layer V	+/+	++	+	-/+	++	++
Neocortex, layer VI	+/+	++	+	-/+	++	++
Piriform cortex	+/+	++++	++/++++	+/+	++/++++	++/++++
Clastrum	+/+	++/+++	–	–	+/+	+/+
<b>Olfactory system</b>						
Olfactory bulb, glomerular layer	+/+	+/+	–	–	–	–
Olfactory bulb, granule cell layer	++/+++	++/+++	+/+	+/+	+	+/+
Anterior olfactory nucleus	+/+	++/+++	-/+++	–	+/+	+/+

*In situ* hybridization signals were determined based on relative optical density of film autoradiograms, as well as silver grain density over cells from emulsion-dipped sections. +++++, Highest levels of labeling; ++++, very high; +++, high; ++, moderate; +, low levels; –, signal very close to background. Multiple designations for a single region indicates heterogeneity of labeling in that area. See Results for details.



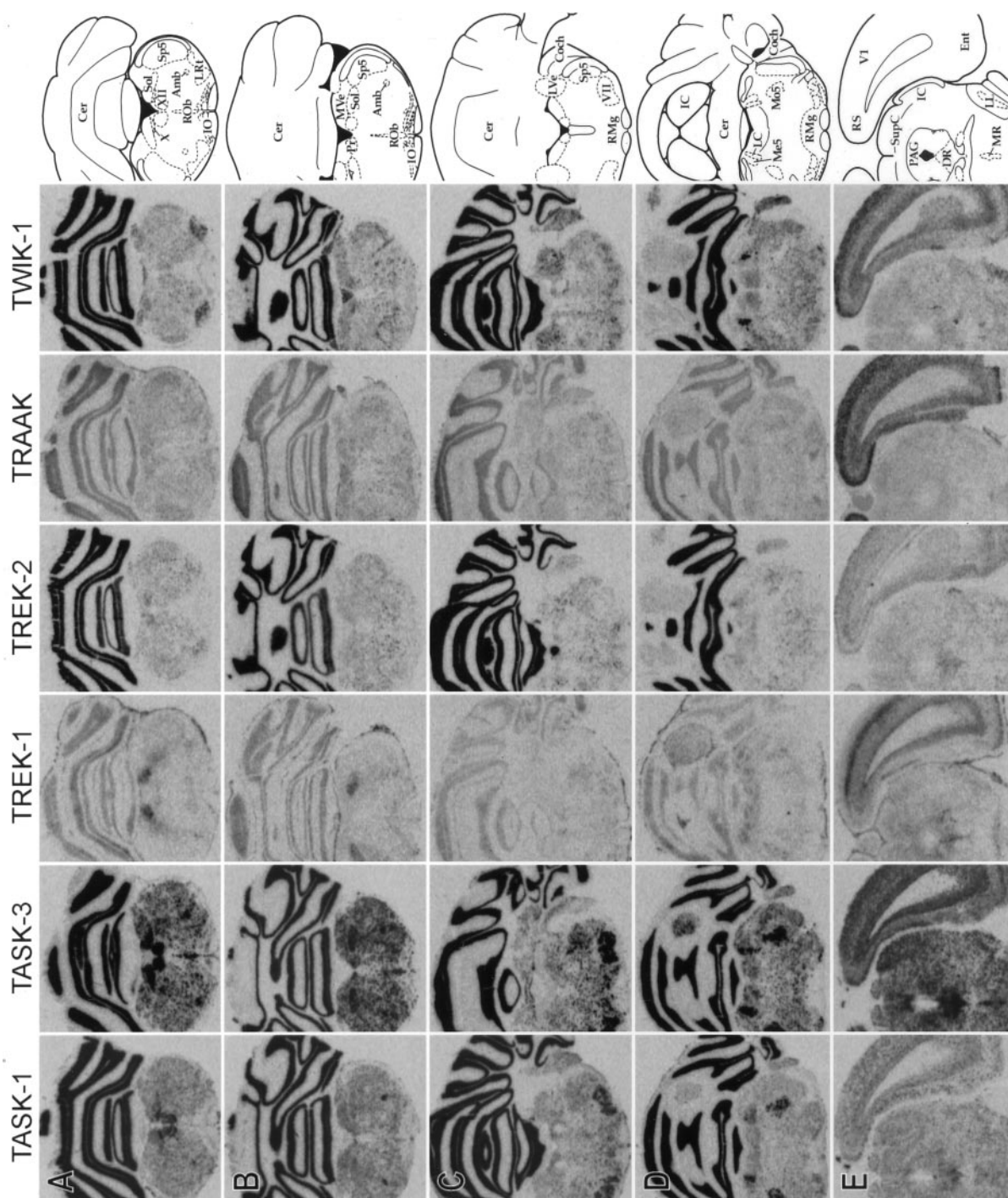


**Figure 1.** CNS distribution of two-pore-domain channels. Coronal sections were hybridized with [<sup>33</sup>P]-labeled cRNA probes for TASK-1, TASK-3, TREK-1, TREK-2, TRAAK, and TWIK-1 and exposed to autoradiographic film. Labeling for TASK-2 in the CNS was uniformly low and therefore is not presented here. Line drawings on the far right are adapted from Paxinos and Watson (1997; reproduced with permission) and indicate the relevant labeled areas. For abbreviations, please refer to Table 2. Scale bar, 3 mm.

expressed (see below). However, only six of the transcripts displayed differential distribution in the CNS. The exception was TASK-2, for which labeling was uniformly low, although the intensity was a little higher than the corresponding sense probe. Because of the low signal and unremarkable pattern of localization, images of TASK-2 in the CNS are not presented.

The relative intensities of labeling of the other six transcripts in the CNS were scored (see Materials and Methods) and are

presented in Table 1. Note that the scoring system and descriptions of the results are based on a comparison of the relative signal intensities not only between different brain regions but also between the various probes. However, it should be understood that the ability to compare levels of different mRNA species (as opposed to levels of the same mRNA in different brain regions) is limited, because there are a number of factors besides cellular mRNA accumulation that can affect hybridiza-

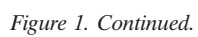


Figure 1. Continued.



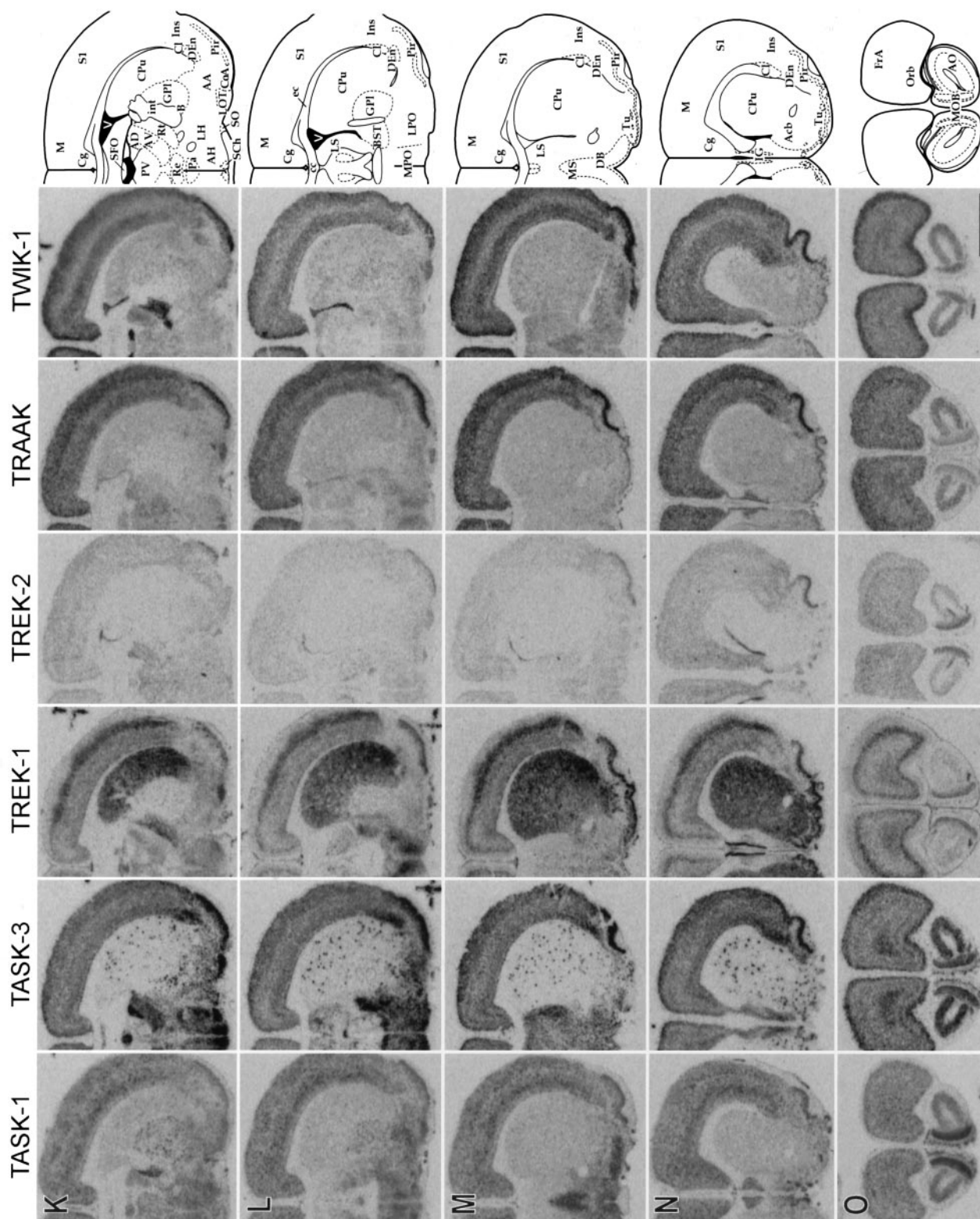


Figure 1. Continued

tion levels, such as the relative hybridization efficiencies of the different probes. Therefore, the results presented here reflect a comparison of mRNA accumulation in different brain regions for each gene considered separately; comparison of signal intensity generated by different probes should be viewed with caution.

### Non-neuronal expression

For all six of the transcripts expressed in the CNS, labeling was consistent with neuronal expression, with the exception of a few regions. This non-neuronal labeling included a number of ventricular structures, such as the choroid plexus (*ChP*), which

**Table 2. Abbreviations**

VII	Facial nucleus	LM	Lateral mammillary nucleus
X	Dorsal motor nucleus	LOT	Nucleus of the lateral olfactory tract
XII	Hypoglossal nucleus	LPO	Lateral preoptic area
AA	Anterior amygdala	LRt	Lateral reticular nucleus
Acb	Accumbens nucleus	LS	Lateral septal nucleus
AD	Anterodorsal thalamic nucleus	LVe	Lateral vestibular nucleus
AH	Anterior hypothalamic area	M	Motor cortex
AHi	Amygdalohippocampal area	MD	Mediodorsal thalamic nucleus
Amb	Nucleus ambiguous	Me5	Mesencephalic trigeminal nucleus
AO	Anterior olfactory nucleus	Me	Medial amygdaloid nucleus
APir	Amygdalopiriform transition area	MG	Medial geniculate nucleus
APT	Anterior pretectal nucleus	MM	Medial mammillary nucleus
Arc	Arcuate nucleus	Mo5	Motor trigeminal nucleus
Au	Auditory cortex	MOB	Main olfactory bulb
AV	Anteroventral thalamic nucleus	MPO	Medial preoptic nucleus
B	Basal nucleus	MR	Median raphe nucleus
BL	Basolateral amygdaloid nucleus	MS	Medial septal nucleus
BST	Bed nucleus of the stria terminalis	MVe	Medial vestibular nucleus
CA1	Field CA1 of hippocampus	Orb	Orbital cortex
CA2	Field CA2 of hippocampus	Pa	Paraventricular hypothalamic nucleus
CA3	Field CA3 of hippocampus	PAG	Periaqueductal gray
cc	Corpus callosum	PF	Parafascicular thalamic nucleus
Ce	Central amygdaloid nucleus	PH	Posterior hypothalamic area
Cer	Cerebellum	Pir	Piriform cortex
Cg	Cingulate cortex	PMCo	Posteromedial cortical amygdaloid nucleus
ChP	Choroid plexus	Pn	Pontine nuclei
Cl	Clastrum	Po	Posterior thalamic nuclear group
CLi	Caudal linear nucleus of the raphe	Pr	Propositus nucleus
CM	Central medial thalamic nucleus	PRh	Perirhinal cortex
CoA	Cortical amygdaloid nuclei	PV	Paraventricular thalamic nucleus
Coch	Cochlear nuclei	R	Red nucleus
CPu	Caudate putamen (striatum)	Re	Reuniens thalamic nucleus
DB	Diagonal band	RMg	Raphe magnus nucleus
DEn	Dorsal endopiriform nucleus	ROb	Raphe obscurus nucleus
DG	Dentate gyrus	RS	Retrosplenial cortex
DM	Dorsomedial hypothalamic nucleus	Rt	Reticular thalamic nucleus
DR	Dorsal raphe nucleus	S	Subiculum
ec	External capsule	S1	Primary somatosensory cortex
Ent	Entorhinal cortex	SCh	Suprachiasmatic nucleus
f	Fornix	SFO	Subfornical organ
FrA	Frontal association cortex	SN	Substantia nigra
GPI	Lateral globus pallidus	SO	Supraoptic nucleus
GPM	Medial globus pallidus	Sol	Nucleus of the solitary tract
Hb	Habenula	Sp5	Spinal trigeminal nucleus
IC	Inferior colliculus	STh	Subthalamic nucleus
IG	Indusium griseum	SuM	Supramammillary nucleus
Ins	Insular cortex	SupC	Superior colliculus
int	Internal capsule	Tu	Olfactory tubercle
IO	Inferior olivary nucleus	V	Ventricle
IP	Interpeduncular nucleus	V1	Primary visual cortex
La	Lateral amygdaloid nucleus	V2	Secondary visual cortex
LC	Locus ceruleus	VL	Ventrolateral thalamic nucleus
LD	Laterodorsal thalamic nucleus	VM	Ventromedial thalamic nucleus
LG	Lateral geniculate nuclei	VP	Ventral posterior thalamic nucleus
LH	Lateral hypothalamic area	VTA	Ventral tegmental area
LL	Nuclei of the lateral lemniscus		

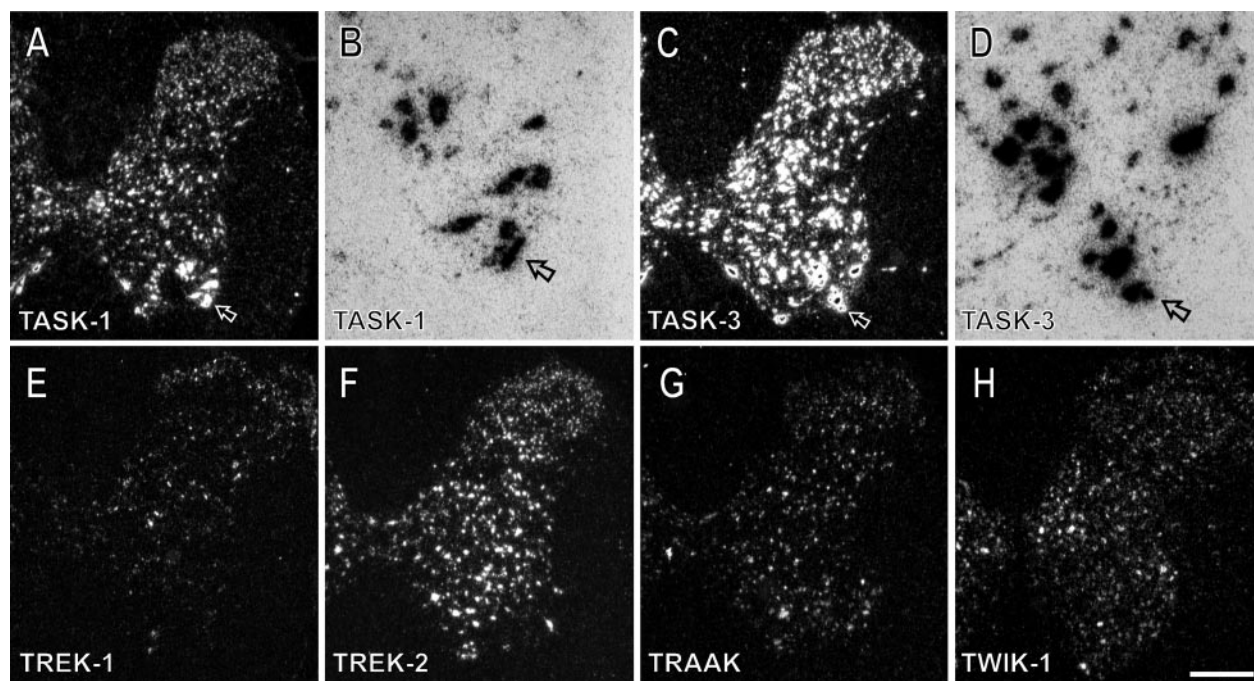


**Figure 2.** Spinal cord expression of two-pore-domain K<sup>+</sup> channel transcripts. Transverse sections from rat cervical spinal cord were hybridized with [<sup>33</sup>P]-labeled cRNA probes and subsequently dipped in liquid autoradiographic emulsion. Silver grains were imaged using dark-field and bright-field microscopy. Top panels (*A–D*) show broad distribution of TASK-1 and TASK-3, with low-to-moderate accumulations of silver grains over many neurons. Ventral horn motoneurons were intensely labeled for both transcripts. In the alternate panels (*B, D*), these same motoneurons are shown at higher power using bright-field optics, with the corresponding cells indicated by *arrows*. Bottom panels (*E–H*) show dark-field images of labeling for the other transcripts in the spinal cord. Labeling for these transcripts was lower, although there were moderate levels of TREK-2 in spinal cord interneuron layers (*F*). Scale bar: *A, C, E–H*, 400  $\mu$ m; *B, D*, 100  $\mu$ m.

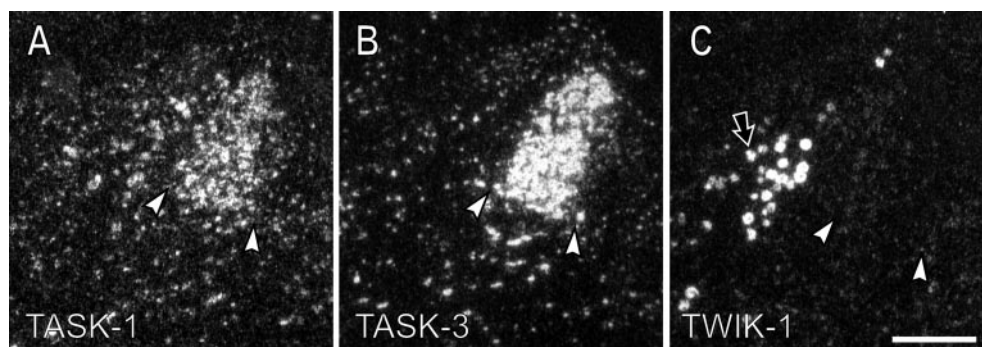


**Figure 3.** TASK-1 and TASK-3 show high levels of mRNA accumulation in the locus ceruleus; TWIK-1 is highly expressed by adjacent mesencephalic trigeminal neurons. Panels show dark-field images of coronal sections through the dorsolateral pons corresponding to autoradiograms in Figure 1*D*. *Arrowheads* in each panel mark the approximate boundary of the locus ceruleus, which had high levels of labeling for TASK-1 (*A*) and was even more densely labeled for TASK-3 (*B*). Large mesencephalic trigeminal neurons are located lateral to the locus ceruleus; these neurons showed high levels of TWIK-1 (*arrow* in *C*). Scale bar, 300  $\mu$ m.

expressed high levels of TWIK-1 (e.g., Fig. 1*H,K,L*; see Fig. 4*G*), the subfornical organ (*SFO*), which expressed high levels of TASK-3 (Fig. 1*K*), and the ependymal cells lining the ventricles, which rostrally expressed moderate-to-high levels of TREK-2 (e.g., Fig. 1*N*) (see Table 2 for a complete list of all abbreviations used). In addition, the pia mater lining the brain contained message for TREK-1; this labeling could be seen in a number of sections (e.g., Fig. 1*A,G*, at the edge of sections) where the pia mater had been left intact during tissue preparation. Aside from these structures, labeling was present in areas rich in neuronal cell bodies but absent in fiber tracts in which only glial labeling is expected (e.g., Fig. 1*L, ec, int, cc*; see Fig. 4).

### Medulla and spinal cord

The medulla and spinal cord were characterized by widespread expression of TASK-3, moderate expression of TASK-1, and generally low expression (with some notable exceptions) of the other transcripts. This was the case in primary sensory areas of the spinal cord and medulla (Figs. 1*A–C*, *Sp5* in the medulla, 2, dorsal horn of the spinal cord), where all transcripts were low except for TASK-1 and TASK-3, which were moderate. Cells of the cochlear nuclei (*Coch*) expressed moderate levels of TASK-1, TASK-3, and TWIK-1 (Fig. 1*C,D*). The nucleus of the solitary tract (*Sol*), which is associated with visceral sensory afferents, had



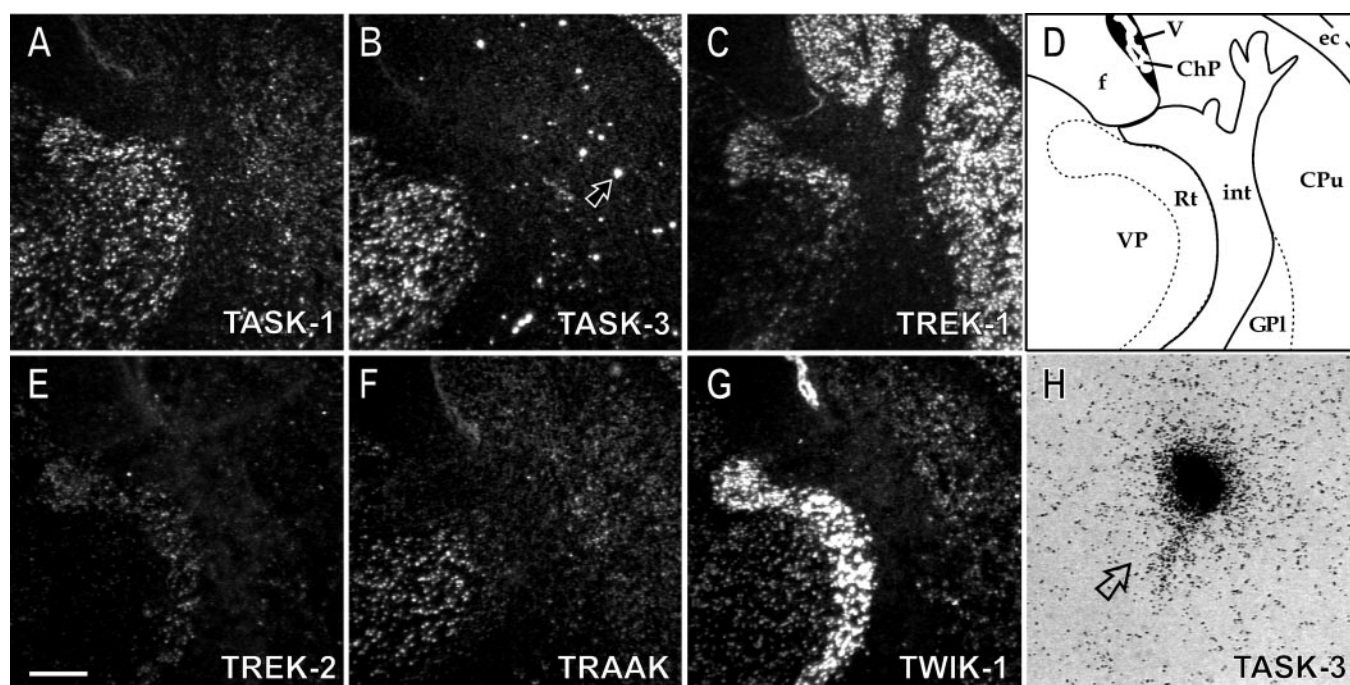


**Figure 4.** Expression of two-pore-domain channels in the thalamus and striatum. Shown are low-power dark-field images of emulsion-dipped sections through the telencephalon, corresponding to the film autoradiograms in Figure 1J. The line drawing (D) indicates the relevant fiber tracts and brain nuclei (for abbreviations, see Table 2). In the caudate putamen, there was uniformly high signal for TREK-1 in cells densely distributed throughout the nucleus (C); these are likely GABAergic output neurons. In contrast, TASK-3 labeled a set of large, sparsely located cells, likely cholinergic interneurons, one of which is marked with an arrow in the dark-field image (B) and in the corresponding high-power bright-field micrograph in H. Also note the intense signal for TWIK-1 in the thalamic reticular nucleus and in the choroid plexus (G). Scale bar: A–G, 500  $\mu$ m; H, 25  $\mu$ m.

moderate-to-high levels of both TREK-1 and TASK-3 (Fig. 1A,B).

Somatic motoneurons expressed high levels of TASK-1 and TASK-3 (Figs. 1A,C,D, 2). Whereas TASK-3 labeling was uniformly strong, TASK-1 was highest in the motor trigeminal (*Mo5*) and in select neurons of the spinal cord (see also Talley et al., 2000). Autonomic motoneurons in the dorsal motor nucleus (*X*) and nucleus ambiguus (*Amb*) also showed high levels of TASK-1 and TASK-3 (Fig. 1A,B).

Neurons in the reticular fields of the medulla and pons (Fig. 1A–E), as well as interneuronal populations of the spinal cord (Fig. 2), contained moderate-to-high levels of mRNA for TASK-3 and moderate levels of TASK-1 but lower levels of the other transcripts. TREK-2 moderately labeled scattered neurons in this region (particularly in the spinal cord) (Fig. 2), as did TWIK-1. This latter transcript was expressed at moderate-to-high levels in the lateral reticular nucleus (Fig. 1A, *LRt*). Neurons of the inferior olive (Fig. 1A,B, *IO*) did not express appreciable levels of any of the transcripts.

### Brainstem aminergic nuclei

Raphe nuclei, which contain serotonergic neuronal cell bodies, showed particularly high expression of TASK-3. This was evident in both the pons (Fig. 1E, *DR*, *MR*) and the medulla (Fig. 1A,B, *ROb*, *RMg*). Low-to-moderate levels of TASK-1 were found in these regions; this was also the case for TREK-1 in the dorsal raphe nucleus (*DR*). The locus ceruleus (*LC*), which contains noradrenergic cell bodies, also was characterized by high levels of TASK-3 and TASK-1 mRNA (Figs. 1D, 3). Note that this nucleus is flanked laterally by mesencephalic trigeminal (*Me5*) neurons, which expressed high levels of TWIK-1 (Figs. 1D, 3; see below). In contrast to the raphe nuclei and the locus ceruleus, dopami-

nergic neurons of the substantia nigra (*SN*) were virtually unlabeled by these transcripts, with the exception of very low levels of TASK-3 and TWIK-1 (Fig. 1F,G). The ventral tegmental area (*VTA*), which also contains dopaminergic neurons, showed moderate labeling for TASK-3 (Fig. 1F).

### Midbrain and cerebellum

Other regions of the midbrain also were characterized by substantial levels of TASK-3 mRNA accumulation. These included the inferior colliculus (Fig. 1D,E, *IC*), the red nucleus, *R*, which also had low-to-moderate levels of TWIK-1 and TREK-2 (Fig. 1F), and the pontine nuclei, *Pn*, which also had high levels of TASK-1 and moderate levels of TWIK-1 (Fig. 1F). There was very high labeling for TASK-3 in the periaqueductal gray (*PAG*); this was particularly evident in the dorsal region (Fig. 1E,F). The interpeduncular nucleus (*IP*) was labeled by high levels of both TASK-1 and TASK-3, as well as moderate levels of TREK-1 (Fig. 1F). Two midbrain cell groups were notable for their high levels of expression of TWIK-1. One was the mesencephalic trigeminal nucleus (*Me5*) (Figs. 1D, 3; noted above). This nucleus contains very large cell bodies of primary afferent neurons, which are similar in function to neurons of the dorsal root ganglia. Notably, some of the very large cells in the dorsal root ganglia also expressed high levels of TWIK-1 (see below). The other midbrain region expressing high levels of TWIK-1 was the superior olivary complex (data not shown).

In contrast to the marked differential expression of the CNS two-pore-domain channel transcripts in most brain regions, the granule cell layer of the cerebellum (*Cer*) was characterized by expression of all six genes (Fig. 1A–E). This expression was extremely high for TASK-1, TASK-3, TREK-2, and TWIK-1 and lower but still appreciable for TREK-1 and TRAAK. TWIK-1

also was expressed in Purkinje cells and in neurons of the deep cerebellar nuclei (data not shown); this latter expression was similar to that of the adjacent vestibular nuclei (Fig. 1C, *Lve*).

### Hypothalamus

The hypothalamus had extremely high levels of TASK-3 in certain nuclei, along with high levels of TASK-1 and TREK-1. Labeling for TASK-3 was particularly intense in the dorsomedial nucleus (*DM*) and the arcuate nucleus (*Arc*) (Fig. 1H,I), the suprachiasmatic nucleus (Fig. 1K, *SCh*), and lateral portions of the mammillary bodies (Fig. 1G, *LM*). It also was high, but less dramatically so, in the medial portion of the mammillary bodies (Fig. 1G, *MM*), as well as in the medial preoptic nucleus (Fig. 1L, *MPO*). Moderate levels were seen in the lateral hypothalamic (Fig. 1G–K, *LH*) and lateral preoptic areas (Fig. 1L, *LPO*) and in the ventromedial (Fig. 1I, *VM*) and paraventricular (Fig. 1J, *K, Pa*) nuclei. TASK-1 had a similar distribution to TASK-3: highest in the dorsomedial and arcuate nuclei (Fig. 1H,I); in the lateral portions of the mammillary bodies (Fig. 1G), and in the medial preoptic nucleus (Fig. 1L), but at lower intensity levels. TREK-1 also was high in the medial preoptic nucleus (Fig. 1L) and the arcuate nucleus (Fig. 1H,I) and moderate in the dorsomedial and ventromedial nuclei (Fig. 1H,I). Expression of both TWIK-1 and TREK-2 was low in the hypothalamus. TRAAK also was low, with the exception of moderate expression in the ventromedial nucleus (Fig. 1I) and suprachiasmatic nucleus (Fig. 1K).

### Thalamus

In the thalamus, the principal relay nuclei had low-to-moderate levels of all of the transcripts except TASK-3. This transcript was moderate-to-high in most relay nuclei, including the medial geniculate (*MG*), posterior (*Po*), ventral posterior (*VP*), laterodorsal (*LD*), and anterodorsal (*AV*) nuclei (Figs. 1F–K, 4). However, labeling for TASK-3 was high in the ventral portion of the lateral geniculate nucleus (Fig. 1G,H, *LG*) and was especially prominent in the anterodorsal nucleus (Fig. 1J,K, *AD*). TASK-1 was higher in the intralaminar thalamic nuclei, especially in the central medial and reuniens nuclei (Fig. 1I,J). TWIK-1 was found at very high levels in the thalamic reticular nucleus (*Rt*), which forms a shell of GABAergic interneurons surrounding the relay nuclei (Figs. 1I–K, 4). In addition, this nucleus had moderate levels of TASK-1 and TREK-1 (Figs. 1I–K, 4). TWIK-1 also was extremely high in the medial habenula (Fig. 1H–J), although it should be noted that this labeling primarily was restricted to the ventral portion of the medial nucleus. Finally, there also was notable labeling for TWIK-1 in the parafascicular thalamic nucleus (Fig. 1H, *PF*).

### Basal forebrain and amygdala

The basal ganglia were characterized by high expression of TREK-1 and TASK-3; these two transcripts were distributed in the striatum (*CPu*) in a manner consistent with two distinctive cell types (Figs. 1I–N, 4). TREK-1 was evenly expressed at high levels across the striatum. This dense and relatively uniform expression is consistent with localization in GABAergic output neurons, which constitute the vast majority of striatal neurons. In contrast, TASK-3 was expressed by larger, much more sparsely distributed cells, a characteristic of cholinergic striatal interneurons. For both TASK-3 and TREK-1, their respective distribution patterns extended into the accumbens nucleus (*Acb*) and the olfactory tubercle (*Tu*) (Fig. 1M,N). Expression of the other transcripts in these regions was low,

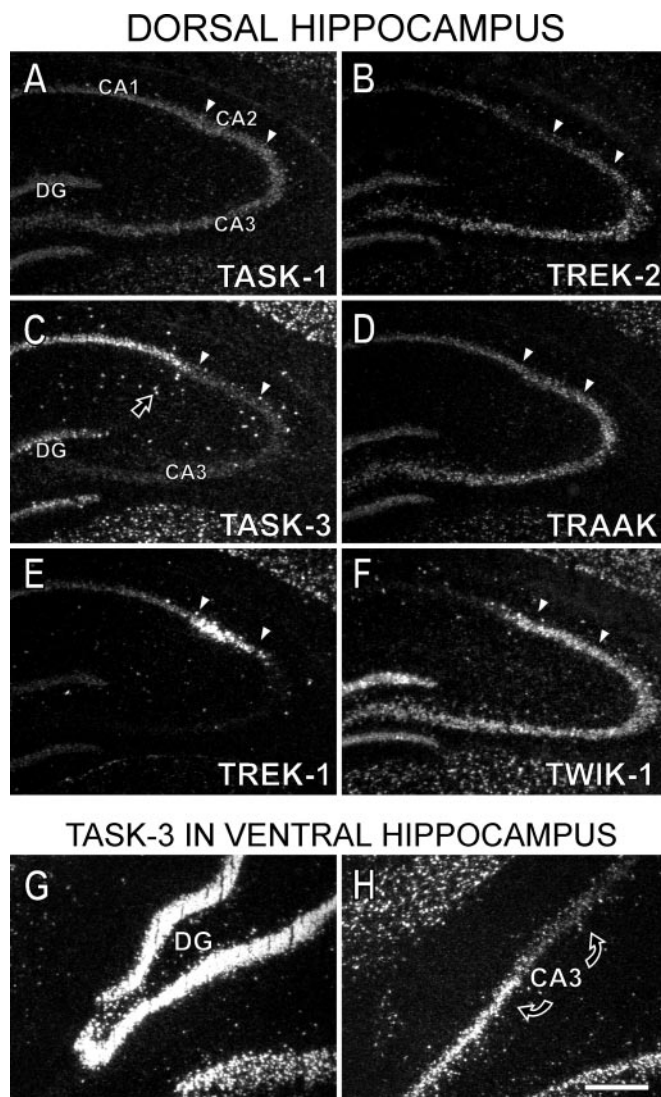


**Figure 5.** Expression of two-pore-domain channels in different regions of the hippocampus. Low-power dark-field images of emulsion-dipped coronal sections through the hippocampus. A–F show labeling for the six channel mRNAs through the rostral/dorsal hippocampus; this view corresponds to the film autoradiograms seen in Figure 1I. Note the differential distribution through the various pyramidal cell populations (CA1, CA2, and CA3), the approximate boundaries of which are marked by arrowheads. Also, there was TASK-3 labeling in scattered cells of the nonpyramidal layers (arrow in C); these are likely hippocampal interneurons. G and H illustrate differential TASK-3 expression in the ventral/caudal hippocampus compared with the rostral/dorsal expression illustrated above. G shows TASK-3 expression in the ventral/caudal dentate gyrus and corresponds to the ventral portion of the film autoradiogram in Figure 1F. Note that there was particularly intense labeling of dentate gyrus granule cells in the ventral hippocampus but very little expression by these cells in the dorsal hippocampus (C). H shows TASK-3 expression in the ventral/caudal portion of CA3 and is taken from a section corresponding to the film autoradiogram seen in Figure 1G. The CA3 pyramidal cell layer is marked by curved arrows and traverses the entire panel. Note that there is much more TASK-3 expression in cells in the bottom (i.e., ventral) part of this panel when compared with cells in the top part of the panel and when compared with TASK-3 labeling in CA3 of the dorsal hippocampus (C). Scale bar, 500  $\mu$ m.

with the exception of TASK-1 in the olfactory tubercle, where it was expressed at moderate-to-high levels in some of the cellular islands (Fig. 1N).

It should be noted that the scattering of TASK-3-labeled neu-



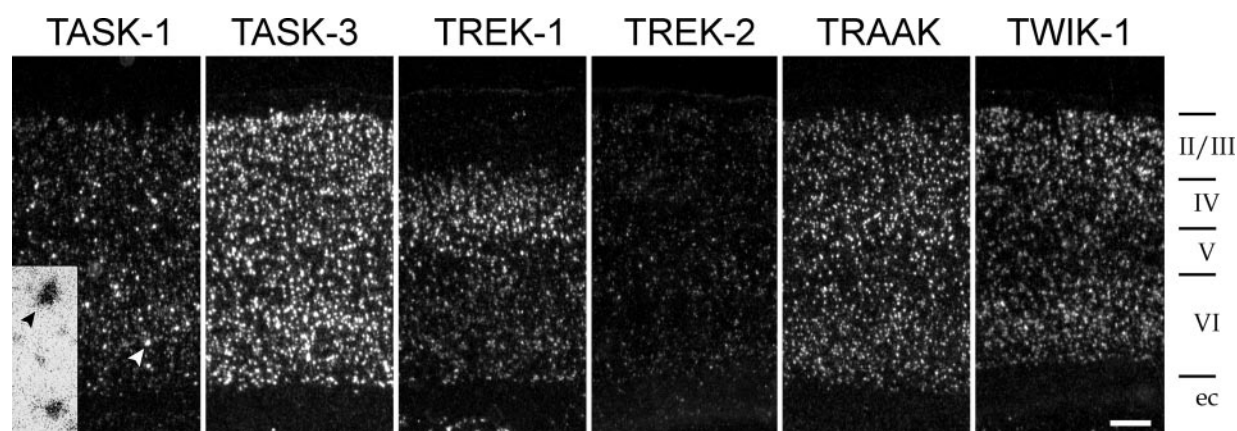


**Figure 6.** Laminar distribution of two-pore-domain K<sup>+</sup> channel transcripts in the neocortex. Shown are dark-field micrographs of the somatosensory cortex. The relevant cell body layers (i.e., layer II through layer VI) are indicated on the right, as is the underlying fiber tract [external capsule (*ec*)]. TASK-3, TRAAK, and TWIK-1 could be seen at appreciable levels in all layers, whereas TREK-1 was highly enriched in layer IV. TASK-1 was expressed at higher levels in a scattering of cells, mostly in layers IV and VI. One of these layer VI cells is marked by an arrowhead and is shown using high-power bright-field optics in the inset on the left. Scale bar: 250  $\mu$ m; inset, 50  $\mu$ m.

rons seen in the striatum extended into the region of the basal nucleus (*B*), just lateral to the internal capsule (*int*), and in the medial portion of the lateral globus pallidus (*GPI*) (Fig. 1*J,K*). This pattern once again is consistent with TASK-3 expression in neurons of a cholinergic phenotype, because the basal nucleus contains a diffuse collection of large (cortically projecting) cholinergic neurons (Fig. 1*J,K*). TASK-1 labeling was present at low-to-moderate levels in the lateral globus pallidus (Fig. 1*J-L*), although in contrast to TASK-3, this labeling appeared to be uniform throughout the nucleus. Also with regard to the globus pallidus, TASK-3 and TWIK-1 were expressed at moderate levels in the medial segment (Fig. 1*J, GPm*). Finally, the subthalamic nucleus (*STh*), another nucleus of the basal ganglia, was characterized by high levels of TASK-3 and moderate levels of TASK-1 and TWIK-1 (Fig. 1*H*).

In the more medial nuclei of the basal forebrain, the bed nucleus of the stria terminalis (*BST*) contained cells expressing high levels of TASK-3 and low-to-moderate levels of TASK-1 and TREK-1 (Fig. 1*L*). There were moderate levels of TASK-3 in the lateral septum (*LS*) and moderate levels of TASK-1 in the medial septum (*MS*) and diagonal band (*DB*) (Fig. 1*M*).

In the amygdala, labeling was highest in the cortical nuclei situated along the ventrolateral surface of the forebrain (Fig. 1*F-K*). Caudally, these included the amygdalopiriform transition area (Fig. 1*F,G, APir*) and the amygdalohippocampal area (Fig. 1*H, AHi*), both of which had high levels of TASK-3 and TWIK-1 and moderate levels of TASK-1, TREK-2, and TRAAK. TASK-3 and TWIK-1 also were high in the rostral cortical amygdaloid nuclei (Fig. 1*J,K, CoA*), whereas the other transcripts were more moderately expressed. The nucleus of the lateral olfactory tract (*LOT*), which is at the rostral end of the amygdala (Fig. 1*K*), had high levels of TASK-3 and TREK-1 and moderate levels of TRAAK. The other area of note in the amygdala was the medial nucleus (Fig. 1*I,J, Me*). TASK-3, TREK-1, and TREK-2 all were more highly enriched in the posterior part of this nucleus, with TASK-3 at particularly high levels. There was low-to-moderate labeling throughout the nucleus for TASK-1, TRAAK, and TWIK-1.

### Hippocampus

Hippocampal pyramidal neurons expressed all transcripts but with differences in distribution (Figs. 1*F-J, 5*). TASK-1 and

TRAAK were low-to-moderate, with relatively even levels of expression throughout. In contrast, TWIK-1 showed moderate labeling in CA2 and CA3 but low levels in CA1, particularly in the caudal sections (Fig. 1*F-H*). TREK-2 had lower levels of labeling but also showed more expression in CA3 than CA1.

For TASK-3, there was a distinct gradient of expression, with more expression ventrally, particularly in CA3 pyramidal neurons, where expression was moderate-to-high at the most ventral/caudal (i.e., temporal) end of the hippocampus (Figs. 1*G, 5H*) but nearly undetectable at the rostral/dorsal (i.e., septal) end (Figs. 1*H-J, 5C*). This TASK-3 expression gradient was even more dramatic for dentate gyrus (*DG*) granule cells, which were intensely labeled ventrally (Figs. 1*F, 5G*) but had only low densities of silver grains dorsally (Figs. 1*H-J, 5C*).

The distribution of TREK-1 also was interesting; it was low-to-moderate in CA1 and almost absent in CA3 but quite high in CA2 and in a limited region of cells adjacent to the hippocampal commissure (Fig. 1*G-I*, the most medial portion of the hippocampus). These two sets of highly expressing cells were conjoined in the very rostral hippocampus, in a region identified as CA3 (Fig. 1*J*). A potentially related set of cells also expressed high levels of TREK-1: neurons of the indusium griseum (Fig. 1*N, IG*). This structure has been hypothesized to be functionally related to the hippocampus (Paxinos, 1995).

There also was expression by cells (presumably interneurons) in nonpyramidal layers of the hippocampus and in the polymorph layer of the dentate gyrus. This was particularly notable for TASK-3 but also was evident for TASK-1, TREK-1, and TWIK-1 (Fig. 5). This labeling was not noticeably restricted to any particular hippocampal laminae.

### Cerebral cortex

The neocortex was associated with high levels of TASK-3, TRAAK, TWIK-1, and TREK-1 (Figs. 1*E-N, 6*). In the case of these first three genes, there was labeling in all cell body layers. This was in contrast to TREK-1, in which high labeling was restricted to layer IV, and there was virtually no expression in layers II–III. The pattern for TREK-1 was consistent with expression in layer IV granule neurons, inasmuch as it was particularly evident in the primary visual and primary somatosensory cortices (Fig. 1: *E, F, VI; H-N, SI*), which contain a high density of this cell type. TREK-2 was low throughout, although it was somewhat



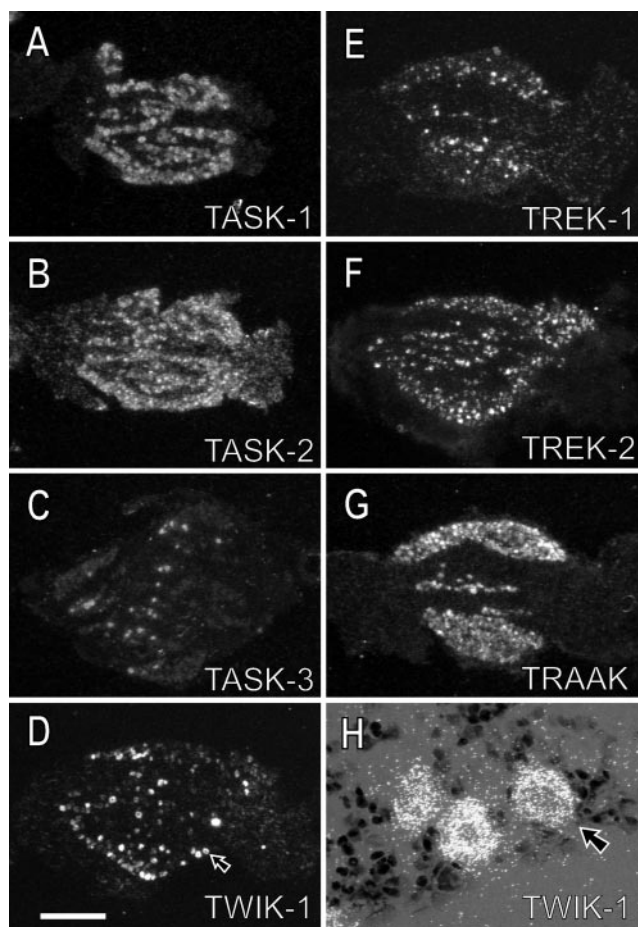


**Figure 7.** Two-pore-domain channel expression in dorsal root ganglia. As shown by dark-field microscopy, all seven transcripts were expressed in dorsal root ganglia, and especially high densities of silver grains were seen for TASK-1 (*A*), TASK-2 (*B*), and TRAAK (*G*). TASK-3 (*C*) was expressed at high levels but by a much more limited proportion of the cells. Labeling for TWIK-1 was for the most part restricted to larger neurons; it is shown at low power in *D*, with a higher-power view of the indicated neuron (*arrows*) shown in *H*. Scale bar: *A–G*, 400  $\mu$ m; *H*, 50  $\mu$ m.

higher in the most caudal (Fig. 1*E*, *VI*, *Ent*) and rostral (Fig. 1*O*, *FrA*, *Orb*) portions of the cortex. This preferential rostral and caudal labeling also was evident in sagittal and horizontal sections (data not shown). TASK-1 was expressed at low-to-moderate levels throughout, but this lower expression was punctuated by a scattering of more heavily labeled cells, especially in layers IV and VI (Fig. 6, *inset*). Also, TASK-3 and TWIK-1 were expressed at higher levels in the outermost layers (II–III) in the motor cortex (Fig. 1*I–N*, *M*) and in the frontal association cortex (Fig. 1*O*).

The allocortex, including cortices on the midline (Fig. 1: *E–J*, *RS*; *K–N*, *CG*) and structures ventral to the neocortex (Fig. 1: *F–I*, *PRh*; *J–N*, *Ins*), showed labeling patterns that were consistent with those of the neocortex, inasmuch as there were high levels of TASK-3, TRAAK, and TWIK-1 and very low levels of TREK-2. There were particularly high levels of labeling in the outermost cell body layers; this pattern was seen for TASK-3, TRAAK, and TWIK-1 in the retrosplenial cortex (Fig. 1*E–J*), for TWIK-1 in the cingulate cortex (Fig. 1*K–N*), and for TASK-3 in the insular cortex (Fig. 1*J–N*). TREK-1 was expressed at low levels in the perirhinal cortex (Fig. 1*F–I*) and was virtually absent from the insular cortex (Fig. 1*J–N*); this once again was consistent with

expression of TREK-1 in layer IV granule neurons of the neocortex, because the perirhinal and insular cortices lack a well developed granule cell layer.

Neurons in the piriform cortex (*Pir*) were remarkable for the fact that they displayed moderate-to-high labeling of all six transcripts (Fig. 1*H–N*). For TREK-1, this labeling was somewhat higher in more rostral sections. Neurons in the claustrum (Fig. 1*K–N*, *Cl*) and the dorsal endopiriform nucleus (Fig. 1*I–N*, *Den*) expressed high levels of TASK-3.

### Olfactory system

In the main olfactory bulb (*MOB*), there once again was substantial overlap of expression (Fig. 1*O*). Labeling was highest for TASK-1 and TASK-3, and these were the only transcripts found at appreciable levels in the glomerular layer. mRNA for all six genes was detected in olfactory granule cells, with TASK-1 and TASK-3 at moderate-to-high levels but with TRAAK at only low levels. Expression in the anterior olfactory nucleus (*AO*) was notable for TASK-1, TASK-3, TRAAK, and TWIK-1. In addition, the external segment of this nucleus (data not shown) expressed high levels of TREK-1.

### Expression in the dorsal root ganglia

As noted, all seven genes were expressed in dorsal root ganglia (Fig. 7). TASK-1, TASK-2, and TRAAK each were expressed by a large proportion of the cells; expression of TREK-1, TREK-2, TASK-3, and TWIK-1 was much more restricted, although for each, there were cells with high levels of expression. Expression of TWIK-1 appeared for the most part to be limited to the very large sensory neurons (Fig. 7*H*), a pattern also seen in sensory neurons of the mesencephalic trigeminal nucleus (Fig. 3).

### KCNK gene expression in the mouse

In addition to the brain sections taken from rat, a few horizontal and sagittal sections were taken from C57BL/6J mice. Also, mouse brainstem and spinal cord slices were taken for analysis of TASK-1, TASK-3, TREK-1, and TRAAK (data not shown). Although a full distribution could not be obtained with these few sections, it was clear that there were no gross differences in the expression patterns, and all of the regions of high expression were identical between the two species. However, a few subtle differences were apparent. For TASK-3, there may have been somewhat less labeling in the thalamus and cerebellum (relative to other brain regions) in the mouse when compared with the rat. Also, the dorsal-to-ventral gradient of TASK-3 expression that was clearly evident in the rat hippocampus (see above) was less apparent in the mouse when comparing expression in sagittal sections (which contained dorsal hippocampus) with horizontal sections (which contained ventral hippocampus). This was also the case for TWIK-1 expression in CA1 pyramidal neurons. In addition, there was moderate TWIK-1 expression in the striatum of the mouse; labeling in this region was low in the rat. There were a couple of slight differences in expression of TRAAK; in the cortex, it appeared that labeling in mouse sections was somewhat higher in the outermost layers compared with the more even laminar distribution of the rat. In the hippocampus, the TRAAK signal was a bit higher in CA3 pyramidal neurons compared with those of CA1; this once again was in contrast to the more even distribution in the rat. No differences were detectable in the distributions of TASK-1, TASK-2, or TREK-2. The patterns of TREK-1 expression were the same for the two species, except that regions of high TREK-1 expression in the rat (e.g., striatum, layer IV of the neocortex, and CA2 pyramidal neurons) were even

more strongly labeled relative to other areas in sections from the mouse.

## DISCUSSION

In this study, we describe the CNS distribution of mRNA encoding seven two-pore-domain potassium channel family members. We found widespread and differential distribution of all transcripts except TASK-2, which was expressed at high levels in the dorsal root ganglia but was present only at uniformly low levels in the CNS. The expression of these KCNK genes was to a large extent complementary; nevertheless, there was substantial overlap of these transcripts in multiple brain areas and likely in individual neurons. Thus, not only do the data suggest that these channels contribute to neuronal diversity, but also that multiple two-pore-domain K<sup>+</sup> channels may provide contributions to the physiological properties and modulatory potential of individual neurons. In addition, the likely coexpression of different subunits suggests the possibility of coassociation (i.e., the formation of heterodimeric channels), particularly by genes that share higher degrees of sequence homology. However, to date there are no reports of heterodimerization among two-pore-domain K<sup>+</sup> channel family members.

Currently, 14 two-pore-domain K<sup>+</sup> channel genes have been identified by molecular cloning, although three (KCNK6/7, THIK-2, and TASK-5) have not generated functional currents in heterologous expression systems (Salinas et al., 1999; Rajan et al., 2000a; Girard et al., 2001; Kim and Gnatenco, 2001). In addition, three (TALK-1, TALK-2/TASK-4, and TASK-5) were cloned very recently from human tissues; they do not appear to be expressed to an appreciable extent in the human brain, and corresponding rodent orthologs have not been identified (Decher et al., 2001; Girard et al., 2001; Kim and Gnatenco, 2001). Of the two remaining genes that we did not examine, TWIK-2 appears to be absent from the rodent brain (Patel et al., 2000). Thus, in the present report, we describe seven of eight functional two-pore-domain potassium channel members with known CNS expression. The exception is the recently cloned THIK-1, which along with the presumed channel THIK-2, is expressed in multiple brain regions in the rat (Rajan et al., 2000a; see below).

### Comparison with previous reports

There have been previous brief descriptions of mRNA expression of these channels in the rodent CNS; our more detailed results are to a large extent in agreement with these reports. As with the current work, two reports on TASK-1 show a predominance of mRNA expression in the cerebellum, in the granule cell layer (Duprat et al., 1997; Brickley et al., 2001). For TASK-2, low levels were seen in the CNS by reverse transcription (RT)-PCR, although in contrast to our results, no expression was seen in dorsal root ganglia (Gray et al., 2000) (but see Medhurst et al., 2001). Also in concordance with our results are two recent abstracts reporting widespread CNS distribution of TASK-3 by *in situ* hybridization, with prominence in many of the same nuclei described here (Rajan et al., 2000b; Vega-Saenz de Miera et al., 2000). Our finding that TREK-2 was primarily restricted to the cerebellum is consistent with previous Northern blot analysis (Bang et al., 2000). Similarly, our findings of high levels of TRAAK in the cerebral cortex and TWIK-1 in the cerebellum and cortex are in concert with previous studies (Lesage et al., 1997; Fink et al., 1998). Also note that a comparison of the current results with studies using Northern blotting and/or RT-PCR of tissues dissected from various human brain regions

(Chapman et al., 2000; Lesage et al., 2000; Medhurst et al., 2001) suggests that there is a substantial degree of conservation of expression between humans and rodents. This was particularly evident when considering regions of maximal expression (TWIK-1, cerebellum; TREK-1, caudate putamen; TASK-1, cerebellum; TASK-2, dorsal root ganglia; and TRAAK, cortex).

There were some discrepancies between the current results and previous work, most notably with regard to TREK-1, which we found to be highest in the striatum, CA2 of the hippocampus, and layer IV of the neocortex. This is in contrast to a previous report in which levels in the striatum were unremarkable, and there was uniform labeling of hippocampal pyramidal neurons and in the various cortical laminae (Fink et al., 1996). The reasons for these and other discrepancies are not clear, although it should be pointed out that the distributions we observed were consistent for rat (using two different strains) and mouse. Furthermore, we used a number of different controls (see Materials and Methods), including the use of multiple oligonucleotide probes (two oligonucleotides each for TREK-1, TRAAK, and TWIK-1 and three oligonucleotides for TASK-1), each of which yielded a distribution pattern that was identical to those of the corresponding cRNA probes.

There are reports of protein localization using antibodies to a few of these channels, including TRAAK (Bearzatto et al., 2000; Lauritzen et al., 2000; Reyes et al., 2000), TREK-1 (Bearzatto et al., 2000; Hervieu et al., 2001; Maingret et al., 2001), and TASK-1 (Kindler et al., 2000; Millar et al., 2000). Complete agreement between protein and mRNA localization is not to be expected for a number of reasons, including the fact that mRNA in most cases is restricted to the cell soma, whereas protein can be transported to sites far from the origin of synthesis (e.g., the axon terminal). In this regard, there is immunohistochemical evidence that both TRAAK and TREK-1 are targeted in part to axon terminals (Bearzatto et al., 2000) and are present at synaptic and nonsynaptic sites in cerebellar cultures (Lauritzen et al., 2000). Despite this, there are many regions in which TRAAK and TREK-1 immunoreactivity correlate with the mRNA expression that we described here. For TRAAK, cell bodies and neuropil were labeled in multiple areas of the mouse brain (Reyes et al., 2000), including the cerebral cortex, a region where we found high levels of mRNA. There were interesting correlations between TREK-1 mRNA expression and immunoreactivity in a number of areas. For example, intense immunoreactivity was seen in the pyramidal layer in CA2 of the hippocampus (Hervieu et al., 2001), suggesting that the high levels of mRNA expression that we found in these neurons results in protein expression at the cell body and proximal dendrites. Similarly, immunoreactivity was seen on the cell bodies of GABAergic neurons in the striatum (Hervieu et al., 2001), another region with high levels of TREK-1 mRNA.

An antibody to TASK-1 also is available; however, in our own work (E. M. Talley and D. A. Bayliss, unpublished observations) and in a published report (Kindler et al., 2000) (see also Millar et al., 2000), it strongly labeled astrocytes, including those located in fiber tracts such as the external capsule and corpus callosum. As noted (see Results), we found no evidence for TASK-1 mRNA in any fiber tracts. Furthermore, for most neuronal populations, this antibody only gave a faint signal, and there was no labeling of motoneurons, where we found high levels of TASK-1 mRNA and where there is strong evidence for functional expression of TASK-1 at the cell soma (Sirois et al., 2000; Talley et al., 2000). The reasons for these discrepancies are not clear.



## Regions of low expression

There were a number of regions in which there was little expression of any of these transcripts (e.g., the substantia nigra and inferior olivary nucleus). In these and other regions, it is likely that other channels provide requisite K<sup>+</sup> conductances for maintenance of baseline membrane properties. In this regard, it is important to consider the other two-pore-domain family channels that were not a part of this study (see above). Of these, two are known to be expressed in the CNS at appreciable levels, THIK-1 and the presumed channel THIK-2. However, neither of these channels appears to be enriched in regions identified here as showing low expression for other two-pore-domain K<sup>+</sup> channel transcripts (Rajan et al., 2000a). Note also that baseline potassium conductances can receive contributions from members of the K<sub>IR</sub> and K<sub>V</sub> families (for example, see Williams et al., 1988; Karschin et al., 1996). Indeed, a member of the K<sub>V</sub> family (KCNQ1) forms a constitutively active leak channel when coexpressed with certain regulatory subunits (Schroeder et al., 2000; Tinel et al., 2000).

## Functional correlates in the CNS

Our results support the hypothesis that, as a result of selective expression, heterogeneity among two-pore-domain K<sup>+</sup> channels contributes to variation in the physiological properties and modulation of different populations of neurons. Consistent with our results, TASK-like currents have been identified in motoneurons and locus ceruleus neurons, as well as cerebellar granule neurons, by virtue of their sensitivity to pH, anesthetics, and (in the case of granule neurons) the endocannabinoid anandamide (Millar et al., 2000; Sirois et al., 2000; Talley et al., 2000; Maingret et al., 2001). In addition, arachadonic acid, which activates TREK-1, TREK-2, and TRAAK, potentiates baseline K<sup>+</sup> currents in cerebellar granule cells (Lauritzen et al., 2000) and hippocampal pyramidal neurons (Colbert and Pan, 1999). In neurons dissociated from fetal mesencephalon and hypothalamus (Kim et al., 1995), three types of fatty acid- and stretch-activated K<sup>+</sup> channels were identified based on single-channel properties, two of which appear to correspond to TREK-1 and TREK-2, respectively (Fink et al., 1996; Maingret et al., 1999; Bang et al., 2000; Lesage et al., 2000). Also consistent with expression of TREK-1, which is strongly sensitive to temperature changes below 37°C (Maingret et al., 2000), background K<sup>+</sup> currents have been implicated in the actions of cold-responsive sensory neurons of the dorsal root ganglia (Reid and Flonta, 2001). Finally, a host of neuronal types are subject to effects of neurotransmitter inhibition of background K<sup>+</sup> currents (McCormick, 1992; Reklung et al., 2000), although correlation with specific channel types has only been made in the case of motoneurons and cerebellar granule neurons (Millar et al., 2000; Talley et al., 2000).

In addition to endogenous substances, a number of two-pore-domain K<sup>+</sup> channels are responsive to low concentrations of volatile anesthetics such as halothane and sevoflurane (Patel et al., 1999; Gray et al., 2000; Lesage et al., 2000; Rajan et al., 2000a; Sirois et al., 2000). It has been proposed that clinical actions of these compounds may result in part from activation of TASK channels in motoneurons and in locus ceruleus neurons (Sirois et al., 2000), where inhibition of firing would contribute to immobilizing and hypnotic effects, respectively. Also, two-pore-domain channels have been proposed as substrates for neuroprotective agents, including some cellular lipids (Fink et al., 1998; Duprat et al., 2000; Lauritzen et al., 2000; Meadows et al., 2001). Thus, the value of these channels as targets for therapeutically important

compounds already is evident, and the development of more selective agents may be of more than experimental benefit.

## REFERENCES

- Bang H, Kim Y, Kim D (2000) TREK-2, a new member of the mechanosensitive tandem-pore K<sup>+</sup> channel family. *J Biol Chem* 275:17412–17419.
- Beazatto B, Lesage F, Reyes R, Lazdunski M, Laduron PM (2000) Axonal transport of TREK and TRAAK potassium channels in rat sciatic nerves. *NeuroReport* 11:927–930.
- Brickley SG, Revilla V, Cull-Candy SG, Wisden W, Farrant M (2001) Adaptive regulation of neuronal excitability by a voltage-independent potassium conductance. *Nature* 409:88–92.
- Chapman CG, Meadows HJ, Godden RJ, Campbell DA, Duckworth M, Kelsell RE, Murdock PR, Randall AD, Rennie GI, Gloger IS (2000) Cloning, localisation and functional expression of a novel human, cerebellum specific, two pore domain potassium channel. *Brain Res Mol Brain Res* 82:74–83.
- Colbert CM, Pan E (1999) Arachidonic acid reciprocally alters the availability of transient and sustained dendritic K<sup>+</sup> channels in hippocampal CA1 pyramidal neurons. *J Neurosci* 19:8163–8171.
- Decher N, Maier M, Dittrich W, Gassenhuber J, Bruggemann A, Busch AE, Steinmeyer K (2001) Characterization of TASK-4, a novel member of the pH-sensitive, two-pore domain potassium channel family. *FEBS Lett* 492:84–89.
- Duprat F, Lesage F, Fink M, Reyes R, Heurteaux C, Lazdunski M (1997) TASK, a human background K<sup>+</sup> channel to sense external pH variations near physiological pH. *EMBO J* 16:5464–5471.
- Duprat F, Lesage F, Patel AJ, Fink M, Romey G, Lazdunski M (2000) The neuroprotective agent riluzole activates the two P domain K<sup>+</sup> channels TREK-1 and TRAAK. *Mol Pharmacol* 57:906–912.
- Fink M, Duprat F, Lesage F, Reyes R, Romey G, Heurteaux C, Lazdunski M (1996) Cloning, functional expression and brain localization of a novel unconventional outward rectifier K<sup>+</sup> channel. *EMBO J* 15:6854–6862.
- Fink M, Lesage F, Duprat F, Heurteaux C, Reyes R, Fosset M, Lazdunski M (1998) A neuronal two P domain K<sup>+</sup> channel stimulated by arachidonic acid and polyunsaturated fatty acids. *EMBO J* 17:3297–3308.
- Girard C, Duprat F, Terrenoire C, Tinel N, Fosset M, Romey G, Lazdunski M, Lesage F (2001) Genomic and functional characteristics of novel human pancreatic 2P domain K<sup>+</sup> channels. *Biochem Biophys Res Commun* 282:249–256.
- Goldstein SA, Bockenhauer D, O'Kelly I, Zilberberg N (2001) Potassium leak channels and the KCNK family of two-P-domain subunits. *Nat Rev Neurosci* 2:175–184.
- Gray AT, Zhao BB, Kindler CH, Winegar BD, Mazurek MJ, Xu J, Chavez RA, Forsayeth JR, Yost CS (2000) Volatile anesthetics activate the human tandem pore domain baseline K<sup>+</sup> channel KCNK5. *Anesthesiology* 92:1722–1730.
- Hervieu GJ, Cluderay JE, Gray CW, Green PJ, Ranson JL, Randall AD, Meadows HJ (2001) Distribution and expression of TREK-1, a two-pore-domain potassium channel, in the adult rat CNS. *Neuroscience* 103:899–919.
- Karschin C, Dissmann E, Stuhmer W, Karschin A (1996) IRK(1–3) and GIRK(1–4) inwardly rectifying K<sup>+</sup> channel mRNAs are differentially expressed in the adult rat brain. *J Neurosci* 16:3559–3570.
- Kim D, Gnatenco C (2001) TASK-5, a new member of the tandem-pore K<sup>+</sup> channel family. *Biochem Biophys Res Commun* 284:923–930.
- Kim D, Sladek CD, Aguado-Velasco C, Mathiasen JR (1995) Arachidonic acid activation of a new family of K<sup>+</sup> channels in cultured rat neuronal cells. *J Physiol (Lond)* 484:643–660.
- Kim Y, Bang H, Kim D (2000) TASK-3, a new member of the tandem pore K<sup>+</sup> channel family. *J Biol Chem* 275:9340–9347.
- Kindler CH, Pietruck C, Yost CS, Sampson ER, Gray AT (2000) Localization of the tandem pore domain K<sup>+</sup> channel TASK-1 in the rat central nervous system. *Brain Res Mol Brain Res* 80:99–108.
- Lauritzen I, Blondeau N, Heurteaux C, Widmann C, Romey G, Lazdunski M (2000) Polyunsaturated fatty acids are potent neuroprotectors. *EMBO J* 19:1784–1793.
- Leonoudakis D, Gray AT, Winegar BD, Kindler CH, Harada M, Taylor DM, Chavez RA, Forsayeth JR, Yost CS (1998) An open rectifier potassium channel with two pore domains in tandem cloned from rat cerebellum. *J Neurosci* 18:868–877.
- Lesage F, Lazdunski M (2000) Molecular and functional properties of two-pore-domain potassium channels. *Am J Physiol* 279:F793–F801.
- Lesage F, Guillemare E, Fink M, Duprat F, Lazdunski M, Romey G, Barhanin J (1996) TWIK-1, a ubiquitous human weakly inward rectifying K<sup>+</sup> channel with a novel structure. *EMBO J* 15:1004–1011.
- Lesage F, Lauritzen I, Duprat F, Reyes R, Fink M, Heurteaux C, Lazdunski M (1997) The structure, function and distribution of the mouse TWIK-1 K<sup>+</sup> channel. *FEBS Lett* 402:28–32.
- Lesage F, Terrenoire C, Romey G, Lazdunski M (2000) Human TREK2, a 2P domain mechano-sensitive K<sup>+</sup> channel with multiple



- regulations by polyunsaturated fatty acids, lysophospholipids, and Gs, Gi, and Gq protein-coupled receptors. *J Biol Chem* 275:28398–28405.
- Maingret F, Patel AJ, Lesage F, Lazdunski M, Honore E (1999) Mechano- or acid stimulation, two interactive modes of activation of the TREK-1 potassium channel. *J Biol Chem* 274:26691–26696.
- Maingret F, Lauritzen I, Patel AJ, Heurteaux C, Reyes R, Lesage F, Lazdunski M, Honore E (2000) TREK-1 is a heat-activated background K<sup>+</sup> channel. *EMBO J* 19:2483–2491.
- Maingret F, Patel AJ, Lazdunski M, Honore E (2001) The endocannabinoid anandamide is a direct and selective blocker of the background K<sup>+</sup> channel TASK-1. *EMBO J* 20:47–54.
- McCormick DA (1992) Neurotransmitter actions in the thalamus and cerebral cortex and their role in neuromodulation of thalamocortical activity. *Prog Neurobiol* 39:337–388.
- Meadows HJ, Chapman CG, Duckworth DM, Kelsell RE, Murdock PR, Nasir S, Rennie G, Randall AD (2001) The neuroprotective agent sipatrigine (BW619C89) potently inhibits the human tandem pore-domain K<sup>+</sup> channels TREK-1 and TRAAK. *Brain Res* 892:94–101.
- Medhurst AD, Rennie G, Chapman CG, Meadows H, Duckworth MD, Kelsell RE, Gloger II, Pangalos MN (2001) Distribution analysis of human two pore domain potassium channels in tissues of the central nervous system and periphery. *Brain Res Mol Brain Res* 86:101–114.
- Millar JA, Barratt L, Southan AP, Page KM, Fyfe RE, Robertson B, Mathie A (2000) A functional role for the two-pore domain potassium channel TASK-1 in cerebellar granule neurons. *Proc Natl Acad Sci USA* 97:3614–3618.
- Patel AJ, Honore E (2001) Properties and modulation of mammalian 2P domain K<sup>+</sup> channels. *Trends Neurosci* 24:339–346.
- Patel AJ, Honore E, Lesage F, Fink M, Romey G, Lazdunski M (1999) Inhalational anesthetics activate two-pore-domain background K<sup>+</sup> channels. *Nat Neurosci* 2:422–426.
- Patel AJ, Maingret F, Magnone V, Fosset M, Lazdunski M, Honore E (2000) TWIK-2, an inactivating 2P domain K<sup>+</sup> channel. *J Biol Chem* 275:28722–28730.
- Paxinos G (1995) The rat nervous system. San Diego: Academic.
- Paxinos G, Watson C (1997) The rat brain in stereotaxic coordinates. San Diego: Academic.
- Rajan S, Wischmeyer E, Karschin C, Preisig-Muller R, Grzeschik KH, Daut J, Karschin A, Derst C (2000a) THIK-1 and THIK-2, a novel subfamily of tandem pore domain K<sup>+</sup> channels. *J Biol Chem* 275:16650–16657.
- Rajan S, Wischmeyer E, Karschin C, Liu GX, Preisig-Muller R, Daut J, Karschin A, Derst C (2000b) TASK-3, a novel brain-specific tandem pore-domain potassium channel. *Pflügers Arch* 439:R382.
- Reid G, Flonta M (2001) Cold transduction by inhibition of a background potassium conductance in rat primary sensory neurones. *Neurosci Lett* 297:171–174.
- Rekling JC, Funk GD, Bayliss DA, Dong XW, Feldman JL (2000) Synaptic control of motoneuronal excitability. *Physiol Rev* 80:399–410.
- Reyes R, Lauritzen I, Lesage F, Ettaiche M, Fosset M, Lazdunski M (2000) Immunolocalization of the arachidonic acid and mechanosensitive baseline TRAAK potassium channel in the nervous system. *Neuroscience* 95:893–901.
- Salinas M, Reyes R, Lesage F, Fosset M, Heurteaux C, Romey G, Lazdunski M (1999) Cloning of a new mouse two-P domain channel subunit and a human homologue with a unique pore structure. *J Biol Chem* 274:11751–11760.
- Schroeder BC, Waldegger S, Fehr S, Bleich M, Warth R, Greger R, Jentsch TJ (2000) A constitutively open potassium channel formed by KCNQ1 and KCNE3. *Nature* 403:196–199.
- Sirois JE, Lei Q, Talley EM, Lynch C, Bayliss DA (2000) The TASK-1 two-pore domain K<sup>+</sup> channel is a molecular substrate for neuronal effects of inhalation anesthetics. *J Neurosci* 20:6347–6354.
- Talley EM, Lei Q, Sirois JE, Bayliss DA (2000) TASK-1, a two-pore domain K<sup>+</sup> channel, is modulated by multiple neurotransmitters in motoneurons. *Neuron* 25:399–410.
- Tinel N, Diochot S, Borsotto M, Lazdunski M, Barhanin J (2000) KCNE2 confers background current characteristics to the cardiac KCNQ1 potassium channel. *EMBO J* 19:6326–6330.
- Vega-Saenz de Miera E, Ozaita A, Zadina M, Rudy B (2000) Expression of two pore K<sup>+</sup> channels in the CNS. *Soc Neurosci Abstr* 26:685.7.
- Williams JT, Colmers WF, Pan ZZ (1988) Voltage- and ligand-activated inwardly rectifying currents in dorsal raphe neurons *in vitro*. *J Neurosci* 8:3499–3506.